

ARTICLE OPEN



ISG-2: properties of the second International Simple Glass

Joseph V. Ryan¹✉, Nicholas J. Smith², James J. Neeway¹, Joelle T. Reiser¹, Benjamin Parruzot¹, Steve Tietje², Elzbieta Bakowska², Jarrod V. Crum¹ and Robert A. Schaut²

Given the importance of glass materials to society, their durability when exposed to aqueous solutions is a critical area for research, particularly for vitrified radioactive wastes. This spurred an international team to fabricate a standardized composition based on waste immobilization glass called the International Simple Glass (ISG), which has been the subject of numerous experimental and computational studies focused on aqueous corrosion resistance.

With the original batch of ISG nearly depleted, the international team designed and fabricated a standard glass material, ISG-2, where half the Ca in the original composition was replaced with Mg by mole. This paper presents information on both the ISG-2 composition and a new batch with the same nominal composition as the original ISG, designated ISG-1, including their homogeneity, their physical and thermal properties. The results of static alteration experiments are presented as well to provide a baseline for future aqueous corrosion performance investigations.

npj Materials Degradation (2023)7:47; <https://doi.org/10.1038/s41529-023-00352-7>

INTRODUCTION

Glass materials, particularly the most common silicate glasses, are sometimes seen as inert relative to their environment. Geologic and historical glasses have, after all, survived hundreds to millions of years exposed to various environments. This is one major reason that glass has been widely used as a host material to immobilize radioactive wastes and to limit the release of radionuclides into the biosphere. The high chemical durability of borosilicate glass compositions designed for this application complicates their study, however. For instance, direct experimental studies of glass behavior at laboratory time scales cannot be simply extrapolated to performance lifetimes of hundreds to thousands of years. Instead, the chemical and physical mechanisms of corrosion must be studied at a fundamental level in order to achieve an actionable understanding of glass corrosion over any time scale¹. With this mechanistic understanding, models can be developed that calculate the expected extent of degradation that accounts for the environmental conditions an individual glass composition will experience over its useful life².

Another major reason for the use of silicate glasses in the immobilization of nuclear wastes is that the glass can incorporate a wide variety of elemental chemistries and form a stable product. The compositionally diverse glasses in use, however, exhibit substantial differences in glass corrosion behavior, and this has led to studies that, while independently robust, are difficult to directly compare. Thus, the international waste glass corrosion scientific community determined that a common and relatively simple glass composition—one nevertheless still similar to the desired composition space—could enable direct comparison of research results and accelerate the pace of accumulated learnings needed for the development of reliable models for glass corrosion. This motivated the design and fabrication of the original International Simple Glass (ISG): a six-component borosilicate glass composed of Si, B, Na, Al, Ca, and Zr oxides. The composition struck a balance between (a) being comparative to a variety of waste glass compositions under consideration by the international waste glass community, (b) being simple enough for atomistic computer

models, and (c) having aqueous corrosion durability behavior similar to other waste glass compositions of interest. The ISG glass composition has the same molar ratios of the six oxides as is found in the SON68 glass, a non-radioactive simulant glass based on the R7T7 glass composition produced at La Hague in France³.

In 2011, the ISG composition was fabricated by MoSci Corp. into 0.5 kg bars that were subsequently the subject of a multifaceted set of investigations, including physical and mechanical properties, dissolution behavior, and computational modeling (see Reiser et al.⁴, Kaspar et al.⁵, and references therein). The popularity of using this composition in research and its success in corrosion experiments led to a universal desire to continue the general theme as the original 50 kg batch of ISG became depleted. During the annual International Workshop on Long-Term Glass Corrosion in 2019, an international consortium representing five countries (see Supplementary Information, Section 1) voted unanimously that producing more standard glass would be enormously beneficial. Having representatives in the consortium and a long-standing commitment to advancing glass science, Corning Incorporated volunteered to produce this new batch of ISG for the international glass corrosion community at no charge. This production would also make use of a continuous melter at Corning's research facility, enabling the next production of standard glass to have better intra-sample homogeneity, improved sample-to-sample consistency, and a much larger overall production volume to supply the glass corrosion community for years to come. Raw materials with improved purity were also provided by Corning for this production, in order to yield glass with substantially lower impurity levels compared to the previous ISG production. For example, trace levels of Fe were expected from raw materials, as in the original ISG, albeit at a lower level (50 to 200 ppm, as opposed to roughly 650 ppm in the original ISG)⁵. All of these suppositions were verified experimentally and are documented in this report.

In terms of candidate compositions, discussions were held that a simple reproduction of ISG would be sufficient, but two major points served to lessen enthusiasm with this simple approach.

¹Pacific Northwest National Laboratory, Richland, WA 99354, USA. ²Corning Research and Development Corporation, Corning, NY 14831, USA. ✉email: joe.ryan@pnnl.gov

First, although compositions can be nearly duplicated, often the unique thermal history of a glass can produce measurable differences with a new synthesis of the same material. Similar logic applies in subtleties of glass production for reproducing a composition, such as differences in homogeneity, low-level metallic impurities, and water content. Secondly, it was reasoned that more useful and novel information about the nature of glass corrosion could be obtained by pursuing a different composition. These considerations notwithstanding, it was also agreed that the composition of the new standard glass should be related somewhat closely to the original ISG, such that future research could leverage the relationship between the two compositions.

Thus, the consortium decided that two batches should be produced: (1) a reproduction targeting the original ISG composition, designated as ISG-1 to differentiate this newly-synthesized glass batch from the prior production by MoSci Corp., and (2) a new glass composition referred to as ISG-2. The ISG-1 composition replenishes the diminished original ISG stock and enables comparative testing between the original and new composition, as the newer production of ISG-1 would offer improved compositional uniformity and purity relative to the original ISG glass blocks. During the 2019 discussions on the new ISG-2 composition, the consortium decided that ISG-2 should be strongly related to the original ISG composition, but with notable changes that would both alter its dissolution behavior in meaningful ways and establish ties to other glass compositions of interest in the glass corrosion community. In terms of major changes to the composition, five main options were put forward:

- (1) *Increase in SiO₂* relative to other modifying and intermediate species, targeting a more dramatic change in connectivity of the Si-O-Si network, and potentially helping to discriminate between structural regimes that represent a fully-interconnected (or percolated) Si-O-Si network versus one that is not (e.g., the original ISG)^{6,7}.
- (2) *Increase Al₂O₃* from 3.8 mol % to 7 mol % Al₂O₃ and decrease B₂O₃ and remove ZrO₂. An investigation of Al is of interest because of the unique chemistry of Al in the glass (e.g., Al avoidance rule and the need for a charge compensating ion with [AlO₄]⁻) and the interesting observation that increasing Al concentration in the glass results in an increase in durability followed by a decrease in durability if a critical concentration is reached^{4,8–10}.
- (3) *Replace half or all of the CaO in the original ISG composition by MgO.* The Mg role in glass structure and during alteration has long been a focus in the community. It is of particular importance as a major component in certain UK and French nuclear waste glass compositions. Mg is also an important component of key secondary phases (e.g., clays, Mg silicates), that are thought to impact glass dissolution kinetics when present^{11–14}.
- (4) *Investigate glass compositions out of the nuclear waste glass family.* The compositions of the discussed glass families, such as pharmaceutical glasses, would have the same components as ISG (except ZrO₂) with a much higher SiO₂ content and commensurate lower forward rates. These glasses also have sufficient network formers to meet the intent of option 1 (Network Percolation).
- (5) *Produce a simplified version of a different nuclear waste glass analogue.* The APCI glass, a composition previously studied at PNNL was considered for this option^{15,16}.

In each case, the impact of such structural changes on dissolution rates and mechanism could be correspondingly inferred. Potential drawbacks for each option were discussed. For options 1 and 4, the calculations to estimate the targeted network percolation transition points remain under debate, such that an appropriate target might be difficult to design. Many options (1, 2, and 4) would likely result in much slower dissolution

Table 1. Target compositions for ISG-1 and ISG-2 in comparison to original ISG batch (from MoSci).

Species	Batch Target Compositions (this work)				
	Original ISG wt%	ISG-1 wt%	ISG-2 wt%	ISG-1 mol%	ISG-2 mol%
SiO ₂	56.20	56.20	56.54	60.1	60.1
Al ₂ O ₃	6.10	6.10	6.14	3.84	3.84
B ₂ O ₃	17.30	17.30	17.40	15.97	15.97
Na ₂ O	12.20	12.20	12.27	12.65	12.65
MgO	< 0.17	< 0.17	1.80	0	2.86
CaO	5.00	5.00	2.52	5.73	2.87
ZrO ₂	3.30	3.30	3.32	1.72	1.72
La ₂ O ₃		0.12	0.12	0.02	0.02
Sum	100.1	100.22	100.12	100.0	100.0

Highlighted are compositions in both wt% and mol% showing the 50% MgO-for-CaO replacement, on a molar basis, in the target ISG-2 composition.

rates, leading to impractically-long experiment timeframes. Further, options 1, 4, and 5 would represent a significant departure from the composition space seen in most nuclear waste glasses amongst the majority of nations—the last being one of the motivations behind the original ISG target. Following these discussions, a vote was taken and fourteen of the twenty-one voters listed a composition based on the original ISG but with half of the Ca replaced by Mg as their first choice (Option 3), with 4 more voters listing it as their second preference.

After a composition option was selected for ISG-2, discussions focused on dopant additions at a trace level (0.1 wt. %) in the glass, where elements could be added for use as a tracers of network dissolution and retention in the alteration products. Due to process constraints, Mo, a common alternative tracer of network glass dissolution, could not be added. Thus, La was selected to act both as an element fully retained in the amorphous alteration layer and optical dopant for laser-assisted atom probe tomography (APT) analysis¹⁷. The international consortium also decided to add the La tracer to the ISG-1 composition so future efforts with the original composition could exploit its addition.

Based on the above considerations, the final compositions and dopant concentrations of ISG-1 and ISG-2 were decided. Target compositions of the original ISG, ISG-1, and ISG-2 are given in Table 1. Emphasis is placed here on the 50% swap of MgO-for-CaO, on a molar basis in ISG-2, in comparison to the Mg-free composition of the original ISG and ISG-1. Meanwhile the tracer species lanthanum oxide (La₂O₃) was incorporated as a + 0.12 wt. % target addition in addition to the equivalent major oxide composition in wt%. Notable differences in the final compositions of ISG-1 versus the original ISG are discussed in the results section.

In the present paper, the production of ISG-1 and ISG-2 glasses at Corning's facilities is described, including the limited quantity of intermediate compositions between ISG-1 and ISG-2 collected during the composition transition. Additionally, the chemical, thermal, and physical properties of ISG-1 and ISG-2 glasses are summarized in comparison to the original ISG composition. The consistency, homogeneity, and purity of these glass samples is also shown herein to be markedly improved relative to the original ISG samples, and benefits the original goal of the international glass corrosion community to provide consistent, comparative standard materials that enable coordinated research into the fundamental mechanisms of glass corrosion. This work is the next step in the ongoing effort to developing accurate aqueous

corrosion models applicable over wide ranges of environmental conditions and time scales.

RESULTS AND DISCUSSION

The results of the studies are broken into sections on composition, glass quality, physical properties, and dissolution behaviors. In each case, additional data can be found in the Supplementary Information, Section 2, provided with this paper.

Glass composition analyses

Table 2 summarizes results from a series of composition and density measurements performed throughout the course of glass production at Corning. Reported concentrations, in wt%, were determined by XRF, with the exception of B_2O_3 , which was determined by ICP-OES. As an additional reference, a few measurements of transition glasses between the ISG-2 and ISG-1 endpoint compositions are included, with decimal designations indicative of their approximate time of sampling during the transition, i.e., ~25%, ~50% or ~75% between the two endpoints. The transition glasses are referred to, using very approximate percentages, as follows: 75% ISG-1 and 25% ISG-2 is denoted as 'ISG-1.25', while 50% ISG-1 and 50% ISG-2 is 'ISG-1.50', and 25% ISG-1 and 75% ISG-2 is 'ISG-1.75'. Noteworthy in Table 2 is the high level of consistency in glass composition for both ISG-2 and ISG-1

over the entirety of the production, demonstrating essentially no meaningful box-to-box variation for these compositions outside of expected measurement uncertainty. The same consistency is also observed in the measured density values for these glasses. These results help establish a high degree of confidence that the ISG-1 and ISG-2 glass collections are self-consistent, and that different researchers studying these glasses (lots labeled by Box#) will not experience variability arising from box-to-box variations in composition from the produced glasses. A comparison of the XRF/ICP-OES compositional data with that obtained with EPMA is given in Table 3 for ISG-1 and ISG-2, while similar information is available in Table S2 for the other glasses. The two compositional analysis protocols returned very similar results. Data on trace-level impurities, all less than 0.1 wt%, can be found in Table S1.

Glass quality / homogeneity

The presence, frequency, and severity of defects in glass can affect the consistency and accuracy of subsequent corrosion tests. For example, bubbles in the glass can present extra surface area for corrosion and high aspect features that may corrode more rapidly than a flat plate. Similarly, compositional variation, significant stresses, or crystalline inclusions (unmelted or poorly mixed batch) can cause regions of a sample to corrode nonuniformly and introduce error in averaged and normalized results.

Table 2. Analyzed compositions as a function of time during production.

Composition	Box #	Analyzed Glass Compositions (wt%)							Density ($g \cdot cm^{-3}$)	
		Al_2O_3	$B_2O_3^*$	CaO	La_2O_3	MgO	Na_2O	SiO_2		ZrO_2
ISG-2	1	6.0	17.5	2.5	0.10	1.8	12.1	57.0	3.3	2.475
ISG-2	5	6.0	17.4	2.5	0.10	1.8	12.1	57.1	3.3	2.474
ISG-2	10	6.0	17.4	2.5	0.12	1.8	12.1	57.0	3.3	2.475
ISG-2	15	6.0	17.4	2.5	0.13	1.8	12.1	56.9	3.3	2.475
ISG-2	20	6.0	17.4	2.5	0.13	1.8	12.2	56.9	3.3	2.475
(ISG-1.75)	–	6.0	17.4	3.4	0.15	1.1	11.9	56.5	3.3	2.486
(ISG-1.50)	–	6.1	17.2	3.9	0.15	0.8	11.9	56.7	3.3	2.490
(ISG-1.25)	–	6.1	17.3	4.3	0.15	0.5	11.8	56.4	3.3	2.496
ISG-1	1	6.0	17.3	4.9	0.15	0.0	12.1	56.4	3.3	2.508
ISG-1	5	5.9	17.2	4.9	0.15	0.0	12.0	56.5	3.3	2.507
ISG-1	10	6.0	17.3	4.9	0.15	0.0	12.1	56.2	3.3	2.509
ISG-1	15	6.0	17.3	4.9	0.15	0.0	12.0	56.4	3.3	2.508
ISG-1	20	5.9	17.4	4.9	0.15	0.0	12.1	56.3	3.3	2.508

This summary of analyzed compositions as a function of time highlights compositional consistency during production, particularly at the ISG-1 and ISG-2 endpoint compositions. Transition glasses shown with approximate decimal designations. All elements analyzed by XRF, except for B_2O_3 , which was determined by ICP-OES.

Table 3. Analyzed final compositions.

Glass	Technique	Analyzed Glass Composition (wt%)								Total	
		Al_2O_3	B_2O_3	CaO	La_2O_3	MgO	Na_2O	SiO_2	ZrO_2		Others
ISG-1	EPMA	5.8	16.8	4.9	0.14	0.0	11.9	55.5	3.1	0.2	98.3
	XRF + ICP-OES	6.0	17.3	4.9	0.15	0.0	12.0	56.4	3.3	0.2	100.3
ISG-2	EPMA	5.7	16.9	2.5	0.09	1.7	11.9	56.5	3.2	0.2	98.7
	XRF + ICP-OES	6.0	17.4	2.5	0.12	1.8	12.1	57.0	3.3	0.2	100.4

Summary of mean analyzed compositions for ISG-1 and ISG-2 compositions measured across 2 labs. Average over multiple samples, using the indicated analytical techniques.

Visual inspection by trained and qualified operators quantified the number and size of both solid and gaseous defects in original ISG, ISG-1 and ISG-2 glasses. Defect counts were then normalized to the quantity of glass mass inspected (defects per pound of glass). The original ISG contained 1500–2000 bubbles per pound, significant haze, and negligible solid inclusions. ISG-1 and ISG-2 glasses contained 50–100 bubbles per pound, no visible haze, and no solid inclusions. The reduction in haze and bubbles with ISG-1 and -2 relative to the original ISG is shown via edge-lit

photographs of polished plates at the top of Fig. 1, and improved homogeneity and reduced stress is illustrated by birefringence photographs at the bottom of Fig. 1.

Physical properties

The physical properties measured for the new glasses are in close agreement with values measured and reported for the original ISG glass. Table 4 reports the measured viscosity point temperatures, thermal expansion coefficient, density, liquidus temperature, and

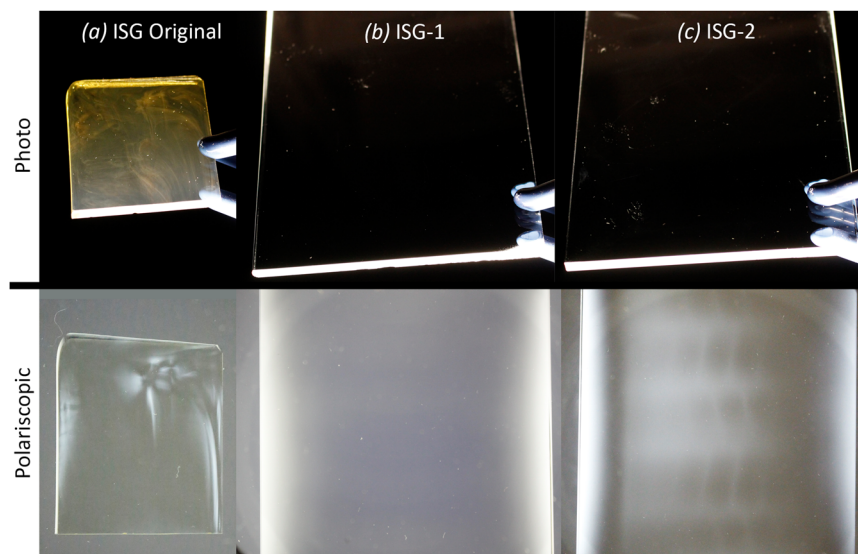


Fig. 1 Homogeneity of glasses. Photographs of ~3.5 mm thick polished slices of original ISG, ISG-1, and ISG-2 with widths of 47 mm, 94 mm, and 94 mm, respectively. At top, the glasses are illuminated by intense edge lighting against a dark background, showing differences in the number of bubbles and the presence of haze between the glasses. At the bottom, the glasses are shown under crossed-plane-polarized light. Non-uniformity in the images show that the original ISG exhibited density variation and stress, mostly near the center of mass. The ISG-1 and ISG-2 were more uniform in stress and composition. ISG-2 showed signs of low-stress patterning from the annealing.

Table 4. Tabulation of physical properties for ISG-1 and ISG-2 in comparison to the original ISG.

Property	Unit	Original ISG	ISG-1	ISG-2
Strain Point (Log 14.68, in P)	°C	529	524	533
Annealing Point (Log 13.18, in P)	°C	566	558	566
Softening Point (Log 7.65, in P)	°C	711	707	707
Log 6 (P) viscosity	°C		781	784
Log 5 (P) viscosity	°C		842	852
Log 4 (P) viscosity	°C		927	945
Log 3 (P) viscosity	°C	1024*	1054	1083
Log 2 (P) viscosity	°C		1267	1306
Coefficient of Thermal Expansion	$\times 10^{-7} \cdot \text{K}^{-1}$		72	69
Density – Archimedes	$\text{g}\cdot\text{cm}^{-3}$	2.50–2.53*	2.508	2.475
Density - He Pycnometry	$\text{g}\cdot\text{cm}^{-3}$	2.51–2.53*	2.512 ± 0.001	2.472 ± 0.002
Liquidus	°C	≈830		≈900
Chemical Durability: Base ^a (ISO 695)	$\text{mg}\cdot\text{dm}^{-2}$ (Class)	92.3 ± 9.0 (A2)	77.6 ± 0.7 (A2)	82.2 ± 0.8 (A2)
Chemical Durability: Acid ^b (DIN 12116)	$\text{mg}\cdot\text{dm}^{-2}$ (Class)		565 ± 1 (S4)	497 ± 13 (S4)
Chemical Durability: Water ^c (ISO 720)	$\mu\text{g}\cdot\text{Na}_2\text{O} \cdot \text{g}\cdot\text{glass}^{-1}$	319 ± 4 (HGA2)	273 ± 4 (HGA2)	135 ± 3 (HGA2)
Chemical Durability: 7-day static test (ASTM C1285-21, PCT-B)	$\text{g} \cdot \text{m}^{-2}$	1.145*	0.89 ± 0.09	1.77 ± 0.2

* - Values taken from Kaspar et al, 2019⁵

^a0.5 M NaOH + 0.25 M Na₂CO₃, 102.5 °C, 180 min

^b6 M HCl, 108 °C, 360 min, reported as half mass-loss (see DIN 12116)

^cDI H₂O, 121 °C, 30 min

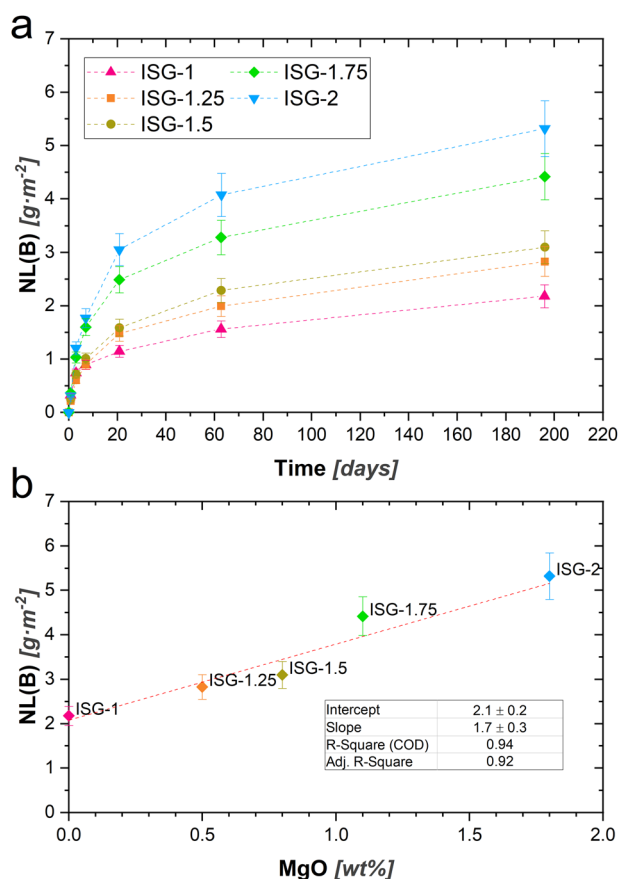


Fig. 2 Release of Boron. **a** NL(B) of the ISG series of glasses. **b** NL(B) at 196 days as a function of Mg content in the glass. The error bars are 1σ and are roughly 10% of the reported value.

several different standard durability values for the original ISG, ISG-1, and ISG-2. Differences in key temperature points between the original ISG and ISG-1 are small, but greater than measurement uncertainty, possibly due to real effect of changing compositions. ISG-2 showed slightly higher temperature points (i.e., more viscous at same temperature) than ISG-1, in accord with general expectations from the replacement of Ca by Mg in its composition¹⁸.

Density measurements of the original ISG match those of ISG-1 within uncertainty, while ISG-2 exhibits significantly lower density by both analytical methods by about 1%. Density measurements for the other glass compositions are provided in Table S3.

Dissolution behavior

Results from standard DIN 12116:2001, ISO 695:1991, and ISO 720:2020 durability tests illustrate that all glasses (original ISG, ISG-1, and ISG-2) are classified similarly within each test; Class S4 performance in concentrated HCl acid, Class A2 performance at high pH, and Class HGA2 performance in high purity hydrothermal water extractions, respectively. The values reported show differences between glass compositions (within the same classifications) but are greater than the standard deviation of the repeat measurements. For acid and neutral water solutions, the results show that durability improves in the order: original ISG, ISG-1, ISG-2.

The static corrosion behavior of the ISG series of glasses is presented in Fig. 2 for the first 196 days of reaction. Figure 2a provides the normalized mass loss of the series of glasses based on boron release. The plots show that the glasses become systematically less durable as the composition transitions from ISG-1 to ISG-2. The results provide insight into the decreased

durability of ISG-2 compared to ISG-1 as NL(B) is roughly 3x higher for ISG-2 compared to ISG-1.

The decrease in durability appears to be linearly dependent on the Mg content (Fig. 2b). The difference in durability does not appear to be due simply to differences in testing pH as pH(T) was the same for all glasses over all time periods (9.0 ± 0.2 , measured pH values for individual tests are provided in Table S4). Additionally, the concentration of Si in the tests (Fig. 3a) appears to be consistent for each test and near the equilibrium concentration of Si for amorphous silica (~120 ppm). These data point to the importance of both the alteration layers and solution [Si] in slowing the glass dissolution rate as the experiment progresses.

Examining the behavior of other elements offers insight into the potential mechanisms that result in a lower durability for ISG-2 relative to ISG-1 as Mg is added through the series. Figure 3b provides the Na retention factor for all glasses as a function of time. In all glass compositions, it is seen that the retention factor is highest at the beginning of the experiment, decreases after about 10 days, then slowly rises through the rest of the test period. Na is known to act as a charge compensator in the alteration layer, as can the other cations, Mg and Ca.

The behavior of these two cations can be examined through the normalized mass loss of Ca and Mg (Fig. 3c and d, respectively). At very short time periods (<10 days) all of the Ca is below the detection limit but the release increases as the experiment progresses. Though there is a high degree of uncertainty in the data because the Ca values are near detection limit, there appears to be a systematic increase in the relative amount of Ca released from the glass as Mg is added into the glass at the expense of Ca. This is the opposite of the effect observed when Ca and Mg are available in solution and Ca retention in the gel layer is favored over Mg¹⁹. The data presented here suggest a preferential incorporation of Mg in the alteration layer or in secondary phases on the altered glass surface relative to Ca. This observation is supported by the data in Fig. 3d, which shows a decreasing normalized loss relative to Mg with increasing Mg content in the glass. Thus, only a relatively small amount of Mg can be released into solution before it is preferentially retained in the alteration layers. Both Mg and Ca have been shown to either incorporate into the gel layer as AlO_4^- charge compensators or precipitate as silicates²⁰. All other sparingly soluble elements (Al, La, Zr,) do not have measurable concentrations in solution so it is not possible to examine their impact on glass corrosion behavior.

The static dissolution behavior of ISG-1 and ISG-2 is also compared to data obtained from similar tests conducted with ISG (Fig. 4a). From the figure, it is observed that the relative durability as measured from NL(B) is slightly higher for ISG-1 compared to ISG whereas ISG-2 is significantly less durable than both versions of the ISG composition. This observation was consistent with 7-d PCT test results (Fig. 4b).

To conclude, the International Simple Glass (ISG), designed in 2010 and synthesized in bulk in 2011, was a successful effort to provide a simple glass composition that could be used as a common reference material for international research efforts into glass corrosion behavior and mechanisms⁵. With the supply of this material diminishing, an effort was undertaken to establish a new supply of reference materials for long- and short-term corrosion research. A variation of the original ISG composition, named ISG-2, has been produced at Corning Incorporated that differs from the original ISG in that half of the CaO has been replaced by MgO on a molar basis. In addition, glass with the same nominal composition as the original ISG, named ISG-1, has been produced to replenish the stock that had been used in the first decade of the international effort to understand glass corrosion. More than 200 kg each of both ISG-1 and ISG-2 were produced, in comparison to the 50 kg of the original ISG material. The glasses were shown to be compositionally uniform within each piece and

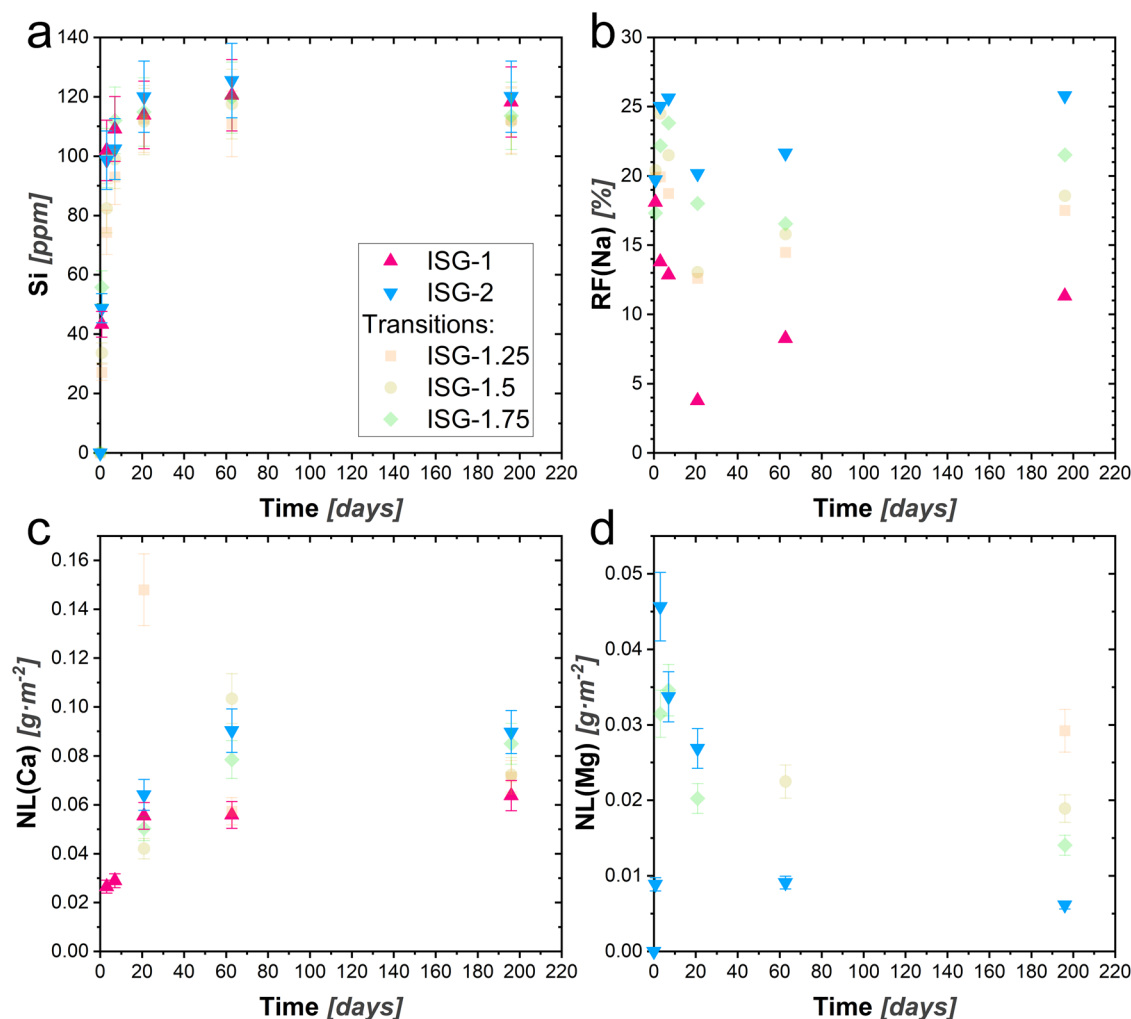


Fig. 3 Release of other elements. Detailed static corrosion results by glass composition including **a** the concentration of Si in solution, **b** the retention factor for sodium, **c** the normalized loss of Ca, and **d** the normalized loss of Mg. The error bars are 1σ and are roughly 10% of the reported value.

consistent across each melt run. The measured compositions were confirmed to be close to each target value, with consensus average compositions given in Table 5. All strips were absent of haze or apparent phase separation and had only 50–100 bubbles per pound.

In static dissolution tests, the extent of glass alteration of ISG-1 was observed to be roughly 90% the extent observed for the original ISG over the same time period. In confirmation of the design goals, ISG-2 was found to exhibit twice the corrosion extent relative to ISG-1 throughout nearly 200 days of testing, which indicates that the presence of MgO at the expense of CaO results in a less durable glass. Further testing with ISG-2 will allow for a more in-depth exploration of the changing corrosion behavior with changes in composition while also providing a reference glass closer in composition and behavior to proposed waste glasses with significant MgO content. Samples of both ISG-1 and ISG-2 can be obtained by contacting the corresponding author.

METHODS

General overview of synthesis procedure

The new glasses were produced at Corning's Sullivan Park research headquarters in Painted Post, NY, using a continuous melter. Batch materials included sand (SiO_2), calcined alumina (Al_2O_3), 5-mol borax ($\text{Na}_2\text{B}_4\text{O}_7 \cdot 5\text{H}_2\text{O}$), soda ash (Na_2CO_3), sodium

nitrate (NaNO_3), magnesia (MgO), limestone (CaCO_3), zirconia (ZrO_2), and lanthanum oxide (La_2O_3). All raw materials were of relatively high purity and batches were mechanically mixed prior to introduction to the melter.

The melter operated continuously (batch being fed, glass being produced) for approximately 2 weeks, during which the process stabilized and glass was routinely characterized to assure that the composition was within tolerances and that glass quality (vis-à-vis homogeneity, defects, dimensions) was adequate. ISG-2 was produced during the first week of melter operation, and then the batch was changed to transition to the ISG-1 composition for the second week. The melt process was held constant (target flow, melting and fining temperatures), with minor adjustments to control glass forming. The melt was mechanically stirred to homogenize any compositional non-uniformity prior to forming. Molten glass was fed to a roller system and rolled in continuous fashion to produce strips of glass approximately 5 mm thick, 90 mm wide, and 300 mm long and then allowed to cool to room temperature. The strips of ISG-2 were uniformly approximately 465 g in mass. Each pedigree of glass (ISG-1, ISG-2, and the select number of transition glasses between ISG-2 and ISG-1) was collected in groupings referred to by Box #, and wherein each box collection occurred within a 24-hour period to ensure consistency within the population.

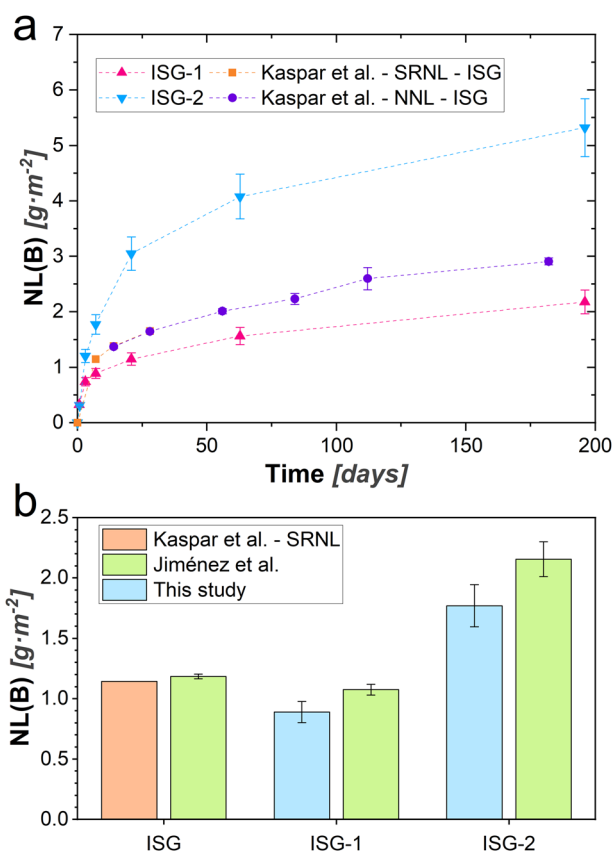


Fig. 4 Comparison to past results. **a** NL(B) of the ISG, ISG-1, and ISG-2 NL(B). **b** a comparison of 7-d release data for ISG, ISG-1, and ISG-2 with other published data^{5,27}. The error bars are 1σ and are roughly 10% of the reported value or are explained in the external references.

The strips were annealed in a separate continuous lehr operation. Glass traveled through a lehr where it was held between strain and anneal temperatures for 45 minutes to relax residual stresses and then cooled slowly to room temperature (Fig. 5).

Composition analyses

X-Ray Fluorescence (XRF) and Inductively-Coupled Plasma Optical Emission Spectroscopy (ICP-OES) were used by Corning to measure the glass compositions produced. XRF samples were core-drilled and polished from the formed strip and measured using a PanAnalytical Axios Max XRF instrument. Quantitation of Al, Ca, Cl, Fe, Hf, K, La, Mg, Na, Si, Sn, Ti, and Zr was possible by use of a multi-standard calibration, and results were expressed as weight percent of the typical oxide (e.g., Fe_2O_3). While XRF can detect B, it is not as reliable as other methods such as ICP-OES. Samples of the glass strips were prepared for ICP-OES analysis by dissolving in HF-based solutions and diluting appropriate to the instrument calibration range. NIST-traceable standards were used for calibration and results were reported as weight percent of B_2O_3 . Boron was the only element reported herein from ICP-OES analysis, and results were treated as interchangeable with the XRF data in examination of the overall glass compositions. Notably, ICP-OES results agreed with XRF within expected uncertainties ($-0.2 / +0.1$), and the summation of all elements were within 0.5 wt% of 100%, implying negligible impact of any subsequent re-averaging and normalization.

The elemental composition of each glass was also measured by electron microprobe analysis (EPMA) at PNNL with a JEOL 8530

HYPERPROBE made by JEOL USA (Peabody, MA). The EPMA uses a field emission gun equipped with five wavelength dispersive spectrometers, each with a take-off angle of 40° . The microprobe data was collected and analyzed with Probe software for EPMA, version 12.6.1, from Probe Software Inc. (Eugene, OR). The microprobe data was collected at an accelerating voltage of 15 kV, beam current of 20 nA, and beam size of $85\ \mu\text{m}$. Oxygen was not directly analyzed and instead was calculated based on stoichiometry of the elemental oxides. The standards and glass samples were coated with 2 nm of iridium to provide a conductive surface and avoid electrical charging. The probe for EPMA software corrected for the effect of the iridium film thickness on the measured elemental concentrations. The samples and standards were analyzed in a group and each sample was analyzed in 5 different locations to find an average and standard deviation of the measured value. Standards (of known concentration) included primary standards for each element, secondary standards for many major components, and interference correction standards. The primary standards were used to find the on-peak positions for each element and to optimize pulse-height analyzer (PHA) settings.

Physical properties

Standard viscosity reference temperatures were determined using standard methods at Corning. Strain and anneal temperatures were determined by fiber elongation methods as described by ASTM C336-71(2020)²¹, as was the softening temperature. Thermal expansion coefficients were measured by dilatometer (ASTM E228)²² and reported as an average value between 0 and 300°C . High-Temperature Viscosity (HTV) measurements were performed using rotating cylinder techniques to capture viscosities below 10^6 poise. NIST-traceable standards are used to minimize bias, which is generally $\pm 5^\circ\text{C}$.

Densities (ρ) of the glasses were measured at PNNL via helium pycnometry on a Micromeritics AccuPyc II 1340 Gas Pycnometer. Ten measurements were performed on a single sample. Densities of the glasses were also measured at Corning via the Archimedes method using deionized water at room temperature according to ASTM C693²³, and results are temperature corrected to 4°C based upon the coefficient of thermal expansion. Stress Optic Coefficient (SOC) or Photoelastic Coefficient (PEC) are determined by diametral compression of a glass cylinder.

Standardized tests of acid, base, and hydrolytic corrosion resistance

Standard durability metrics are commonly used to categorize the general resistance of different glass compositions to acid, base and neutral-pH solutions at Corning. Acid resistance was characterized using boiling 6 M HCl acid and reporting the half-mass loss per unit surface area after 6 h according to DIN12116:2001. Base resistance was characterized using a boiling solution of 0.5 M NaOH and 0.25 M Na_2CO_3 and reported as mass loss per unit surface area after 3 h according to ISO 695:1991. Polished plates approximately 1 mm thick were used in both acid and base measurements. Plates were etched with a HF-HCl mixture according to the standard prior to testing to remove any polishing effects. Hydrolytic Resistance was characterized by titration of glass extracts following a 60-minute exposure to deionized water at autoclave conditions (121°C , 2 atm) according to ISO 720:2020.

Static corrosion testing

The experimental protocol and calculations of the static dissolution experiments conducted at PNNL are given in detail in Parruzot et al. (2019)²⁴ and a summary is given here. The glasses were prepared for static corrosion testing by milling the glass

Table 5. Accepted composition.

Glass	Al ₂ O ₃	B ₂ O ₃	CaO	La ₂ O ₃	MgO	Na ₂ O	SiO ₂	ZrO ₂	Others	Total
Original ISG	5.9	17.7	4.6	–	0.03	12.4	56.3	3.2	0.1	100.0
ISG-1	5.9 ±0.1	17.1 ±0.2	4.9 ±0.1	0.15 ±0.01	0.04 ±0.01	12.1 ±0.1	56.4 ±0.2	3.2 ±0.1	0.2±0.0	100.0
ISG-2	5.9 ±0.1	17.2 ±0.2	2.5 ±0.1	0.11 ±0.02	1.76 ±0.00	12.1 ±0.0	57.0 ±0.3	3.2 ±0.1	0.2 ±0.0	100.0

Consensus values for majors/minors in ISG-1 and ISG-2, in wt%, with ± uncertainty (1 SD). For reference, a typical measured composition of original ISG is listed (Kaspar 2019)⁵.

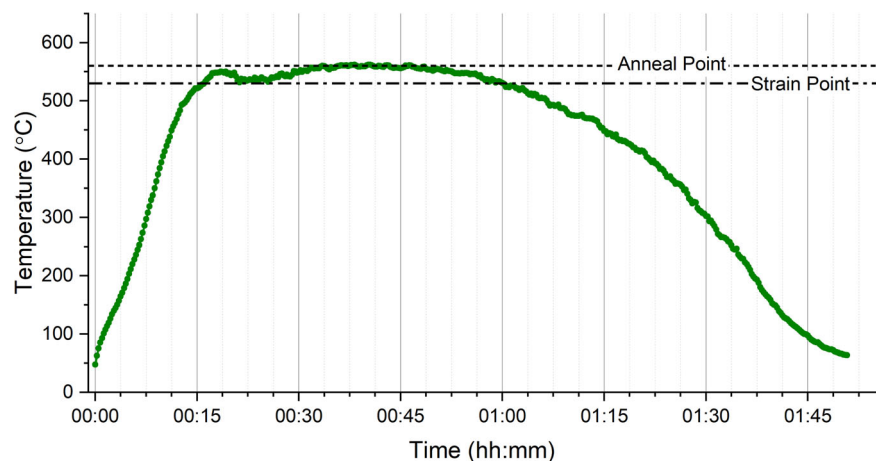


Fig. 5 Thermal profile. Measured thermal profile of the lehr used to anneal all glass strips. Strips were maintained between the strain and anneal temperatures for 45 min to relax residual stresses before slowly cooling to room temperature over more than an hour.

using a tungsten carbide milling chamber, followed by sieving to a size fraction of -100 to +200 mesh (150 to 75 μm). The sieved glass was washed and dried according to ASTM C1285-21²⁵, and a portion of the cleaned glass was verified to be free of fines by scanning electron microscopy.

Crushed glass was loaded into 45 mL 4700 series Parr[®] vessels made of 316 stainless steel. Static experiments were started by adding the target mass of glass powder (≈ 3.5 g), followed by addition of ≈ 37.5 mL ultrapure ASTM D1193-06²⁶ Type 1 water. All tests began at a target glass surface area to solution volume ratio (S/V) of 2000 m^{-1} . Vessels were then sealed and heated in an electric thermostatically controlled oven set to 90 ± 2 °C.

The solutions of the experiments were sampled at 1, 3, 7, 21, 63, and 200 days. Sampling consisted of withdrawing solution aliquots (250 μL) from the reaction vessels using a micropipette. The aliquots were acidified to 3 mL with 0.3 $\text{mol}\cdot\text{L}^{-1}$ HNO_3 (BDH Aristar[®] Plus trace metal grade) for elemental analysis by ICP-OES. Masses of the solution aliquots and nitric acid additions were recorded for each sampling and used instead of solution volume to calculate elemental concentrations. The pH was also measured regularly at the test temperature through the top port, directly in the alteration vessel, with a glass pH electrode (Accumet[™]) calibrated at the same temperature with standard pH buffers.

The vessel mass was recorded before and after sampling to assess any loss caused by evaporation. ASTM Type 1 water was added to the vessel to compensate for solution lost by evaporation only, but not to offset the sampling volume. This was performed when the mass of the solution in the vessel was found to deviate more than 0.5 g from the target solution mass at that time into the experiment.

Acidified solution aliquots were quantitatively analyzed for major element concentrations by ICP-OES using a PerkinElmer Optima[™] 8300 dual-view instrument with an Elemental Scientific

SC4 DX FAST auto-sampler. ICP-OES measurement error was within $\pm 10\%$, the maximum acceptable for calibration verification.

The normalized mass loss values for element i (NL_i) were calculated as described in Parruzot et al.²⁴. The NL_i value compares the relative durability of the different glasses with units of $\text{g}\cdot\text{m}^{-2}$ where g represents the grams of glass normalized to the desired glass constituent, i , and m^2 represents the surface area as the NL_i values are normalized to the sample surface area. Calculations performed here accounted for a decrease in the glass surface area through a shrinking core model as reaction progress increased.

DATA AVAILABILITY

The datasets generated during and/or analyzed during the current study are available from the corresponding author on reasonable request.

Received: 26 August 2022; Accepted: 4 April 2023;
Published online: 06 June 2023

REFERENCES

- Frankel, G. S. et al. Recent Advances in Corrosion Science Applicable To Disposal of High-Level Nuclear Waste. *Chem. Rev.* **121**, 12327–12383 (2021).
- Vienna, J. D., Ryan, J. V., Gin, S. & Inagaki, Y. Current Understanding and Remaining Challenges in Modeling Long-Term Degradation of Borosilicate Nuclear Waste Glasses. *Int. J. Appl. Glass Sci.* **4**, 283–294 (2013).
- Rajmohan, N., Frugier, P. & Gin, S. Composition effects on synthetic glass alteration mechanisms: Part 1. Experiments. *Chem. Geo.* **279**, 106–119 (2010).
- Reiser, J. T. et al. Effects of Al:Si and (Al + Na):Si ratios on the properties of the international simple glass, part I: Physical properties. *J. Am. Ceram. Soc.* **104**, 167–182 (2021).
- Kaspar, T. C. et al. Physical and optical properties of the International Simple Glass. *npj Mat. Deg.* **3**, 15 (2019).

6. Le Losq, C. et al. Percolation channels: a universal idea to describe the atomic structure and dynamics of glasses and melts. *Sci. Rep. -UK* **7**, 16490 (2017).
7. Ojovan, M. I. The Modified Random Network (MRN) Model within the Configurational Percolation Theory (CPT) of Glass Transition. *Ceramics* **4**, 121–134 (2021).
8. Lu, X. et al. Effects of Al:Si and (Al + Na):Si ratios on the properties of the international simple glass, part II: Structure. *J. Am. Ceram. Soc.* **104**, 183–207 (2021).
9. Reiser, J. T. et al. Effects of Al:Si and (Al+Na):Si Ratios on the Static Corrosion of Sodium-Boroaluminosilicate Glasses. *Int J. Appl Glass Sci.* **13**, 94–111 (2022).
10. Vienna, J. D. & Crum, J. V. Non-linear effects of alumina concentration on Product Consistency Test response of waste glasses. *J. Nucl. Mater.* **511**, 396–405 (2018).
11. Abdelouas, A. et al. Surface layers on a borosilicate nuclear waste glass corroded in MgCl₂ solution. *J. Nucl. Mater.* **240**, 100–111 (1997).
12. Fisher, J. G., James, P. F. & Parker, J. M. Soda lime zirconia silicate glasses as prospective hosts for zirconia-containing radioactive wastes. *J. Non-Cryst. Solids* **351**, 623–631 (2005).
13. Góut, T. L., Harrison, M. T. & Farnan, I. Relating Magnox and international waste glasses. *J. Non-Cryst. Solids* **524**, 119647 (2019).
14. Thien, B. M. J. et al. The dual effect of Mg on the long-term alteration rate of AVM nuclear waste glasses. *J. Nucl. Mater.* **427**, 297–310 (2012).
15. Crum, J. V. et al. Baseline Glass Development for Combined Fission Products Waste Streams. Report No. PNNL-18524, (2009).
16. Neeway, J. J. et al. The Dissolution Behavior of Borosilicate Glasses in Far-From Equilibrium Conditions. *Geochim Cosmochim. Acta* **226**, 132–148 (2018).
17. Lu, X. et al. Effects of optical dopants and laser wavelength on atom probe tomography analyses of borosilicate glass. *J. Am. Ceram. Soc.* **100**, 4801–4815 (2017).
18. Kuryaeva, R. G. The state of magnesium in silicate glasses and melts. *Glass Phys. Chem. +* **35**, 378–383 (2009).
19. Debure, M., Frugier, P., De Windt, L. & Gin, S. Borosilicate glass alteration driven by magnesium carbonates. *J. Nucl. Mater.* **420**, 347–361 (2012).
20. Aréna, H. et al. Impact of Zn, Mg, Ni and Co elements on glass alteration: Additive effects. *J. Nucl. Mater.* **470**, 55–67 (2016).
21. ASTM C336-71(2020). Standard Test Method for Annealing Point and Strain Point of Glass by Fiber Elongation, ASTM International, West Conshohocken, PA, (2020).
22. ASTM E228-17. Standard Test Method for Linear Thermal Expansion of Solid Materials With a Push-Rod Dilatometer, ASTM International, West Conshohocken, PA, (2017).
23. ASTM C693-93(2019). Standard Test Method for Density of Glass by Buoyancy, ASTM International, West Conshohocken, PA, (2019).
24. Parruzot, B. P. et al. Multi-glass investigation of Stage III glass dissolution behavior from 22 to 90 °C triggered by the addition of zeolite phases. *J. Nucl. Mater.* **523**, 490–501 (2019).
25. ASTM C1285-21, Standard Test Methods for Determining Chemical Durability of Nuclear, Hazardous, and Mixed Waste Glasses and Multiphase Glass Ceramics: The Product Consistency Test (PCT), ASTM International, West Conshohocken, PA, (2021).
26. ASTM D1193-06. Standard Specification for Reagent Water, ASTM International, West Conshohocken, PA, (2018).
27. Jiménez, J. A., Crawford, C. L. & Lascola, R. J. Physico-chemical properties of international simple glass (ISG) nuclear waste simulants: Luminescence baseline study. *J. Am. Ceram. Soc.* **105**, 1–18 (2022).

ACKNOWLEDGEMENTS

The authors would like to recognize the financial support from Corning leadership to produce these glasses, specifically Charlie Craig and Dr. David Morse. Glass melting

and forming was performed by the Research Melter staff at Sullivan Park, under the leadership of Jim Burns, Jason Frackenpohl and Sean Anderson. The Characterization Sciences group at Corning conducted many of the measurements here, led by Sarah French, Matthew Blodgett, Eileen Fanning, Bailey Flood, Tyler Klein, and Bill Stull. The authors would also like to thank Pacific Northwest National Laboratory (PNNL) staff Steven Baum, Ian Leavy, and Michelle Snyder for their help with ICP-OES analyses of the leachate solutions generated in this study, Ryan Kissinger for collecting the EMPA data, and Daniel Prather for his assistance with the dissolution experiments.

Special thanks go out to the members of the International Workshop on Long-Term Glass Corrosion, both those that directly participated in the ISG-2 selection and all others who have joined the Workshop over the last decade to help define and advance glass corrosion science.

Pacific Northwest National Laboratory is operated for the DOE by Battelle Memorial Institute under Contract DE-AC06-76RLO 1830.

AUTHOR CONTRIBUTIONS

J.V.R. and R.A.S. worked to establish the consensus new glass composition and work out details on its development. The glass synthesis and annealing efforts were directed by R.A.S. and S.T. The various glass property measurements were performed by S.T., E.B., J.T.R., B.P., and J.C. Data interpretation and writing was a joint effort between J.V.R., N.J.S., J.T.R., J.J.N., R.A.S., and B.P.

COMPETING INTERESTS

The authors declare no competing interests.

ADDITIONAL INFORMATION

Supplementary information The online version contains supplementary material available at <https://doi.org/10.1038/s41529-023-00352-7>.

Correspondence and requests for materials should be addressed to Joseph V. Ryan.

Reprints and permission information is available at <http://www.nature.com/reprints>

Publisher's note Springer Nature remains neutral with regard to jurisdictional claims in published maps and institutional affiliations.



Open Access This article is licensed under a Creative Commons Attribution 4.0 International License, which permits use, sharing, adaptation, distribution and reproduction in any medium or format, as long as you give appropriate credit to the original author(s) and the source, provide a link to the Creative Commons license, and indicate if changes were made. The images or other third party material in this article are included in the article's Creative Commons license, unless indicated otherwise in a credit line to the material. If material is not included in the article's Creative Commons license and your intended use is not permitted by statutory regulation or exceeds the permitted use, you will need to obtain permission directly from the copyright holder. To view a copy of this license, visit <http://creativecommons.org/licenses/by/4.0/>.

© Battelle Memorial Institute and Corning Research & Development Corp. 2023